Multi-element fiber technology for space-division multiplexing applications

S. Jain,* V. J. F. Rancaño, T. C. May-Smith, P. Petropoulos, J. K. Sahu, and D. J. Richardson

Optoelectronics Research Centre, University of Southampton, Southampton, S017 1BJ, UK
**sj3g11@orc.soton.ac.uk*

Abstract: A novel technological approach to space division multiplexing (SDM) based on the use of multiple individual fibers embedded in a common polymer coating material is presented, which is referred to as Multi-Element Fiber (MEF). The approach ensures ultralow crosstalk between spatial channels and allows for cost-effective ways of realizing multi-spatial channel amplification and signal multiplexing/demultiplexing. Both the fabrication and characterization of a passive 3-element MEF for data transmission, and an active 5-element erbium/ytterbium doped MEF for cladding-pumped optical amplification that uses one of the elements as an integrated pump delivery fiber is reported. Finally, both components were combined to emulate an optical fiber network comprising SDM transmission lines and amplifiers, and illustrate the compatibility of the approach with existing installed single-mode WDM fiber systems.

OCIS codes: (060.2280) Fiber design and fabrication; (060.2320) Fiber optics amplifiers and oscillators

References and links

1. D. J. Richardson, J. M. Fini, and L. E. Nelson, "Space-division multiplexing in optical fibres," Nat. Photonics **7**(5), 354–362 (2013).
2. R. W. Tkach, "Scaling optical communication for the next decade and beyond," Bell Labs Tech. J. **14**(4), 3–9 (2010).
3. Y. Awaji, K. Saitoh, and S. Matsuo, "Transmission systems using multicore fibers," in *Optical Fiber Telecommunications Volume VI-B: Systems and Networks,* I. P. Kaminov, T. Li, and A. E. Wilner, eds. (Elsevier, 2013), pp. 617–652.
4. K. Imamura, K. Mukasa, and T. Yagi, " Effective space-division multiplexing by multi-core fibers," in *European Conference on Optical Communications* (2010), P1.09.
5. M. Koshiba, K. Saitoh, and Y. Kokubun, "Heterogeneous multi-core fibers: proposal and design principle," IEICE Electron. Express **6**(2), 98–103 (2009).
6. Y. Kokubun and M. Koshiba, "Novel multi-core fibers for mode division multiplexing: proposal and design principle," IEICE Electron. **6**(8), 522–528 (2009).
7. T. Hayashi, T. Taru, O. Shimakawa, T. Sasaki, and E. Sasaoka, "Design and fabrication of ultra-low crosstalk and low-loss multi-core fiber," Opt. Express **19**(17), 16576–16592 (2011).
8. C. Xia, R. Amezcua-Correa, N. Bai, E. Anotnio-Lopez, D. M. Arroija, A. Schulzgen, M. Richardson, J. Liñares, C. Montero, E. Mateo, X. Zhou, and G. Li, "Hole-assisted few-mode multicore fiber for high-density space-division multiplexing," IEEE Photonics Technol. Lett. **24**(21), 1914–1917 (2012).
9. J. Sakaguchi, B. J. Puttnam, W. Klaus, Y. Awaji, N. Wada, A. Kanno, T. Kawanishi, K. Imamura, H. Inaba, K. Mukasa, R. Sugizaki, T. Kobayashi, and M. Watanabe, "19-core fiber transmission of 19x100x172-Gb/s SDM-WDM-PDM-QPSK signals at 305Tb/s," in *Optical Fiber Communications* (2012), PDP5C.1.
10. B. Zhu, T. F. Taunay, M. Fishteyn, X. Liu, S. Chandrasekhar, M. F. Yan, J. M. Fini, E. M. Monberg, and F. V. Dimarcello, "112-Tb/s space-division multiplexed DWDM transmission with 14-b/s/Hz aggregate spectral efficiency over a 76.8-km seven-core fiber," Opt. Express **19**(17), 16665–16671 (2011).
11. R. R. Thomson, H. T. Bookey, N. D. Psaila, A. Fender, S. Campbell, W. N. Macpherson, J. S. Barton, D. T. Reid, and A. K. Kar, "Ultrafast-laser inscription of a three dimensional fan-out device for multicore fiber coupling applications," Opt. Express **15**(18), 11691–11697 (2007).
12. J. Sakaguchi, B. J. Puttnam, W. Klaus, Y. Awaji, N. Wada, A. Kanno, and T. Kawanishi, "Large-scale space division multiplexed transmission through multi-core fiber," in *Asia Communications and Photonics Conference* (2012), AS2C.5.

#200150 - $15.00 USD Received 11 Nov 2013; revised 27 Jan 2014; accepted 4 Feb 2014; published 11 Feb 2014

13. K. S. Abedin, T. F. Taunay, M. Fishteyn, M. F. Yan, B. Zhu, J. M. Fini, E. M. Monberg, F. V. Dimarcello, and P. W. Wisk, "Amplification and noise properties of an erbium-doped multicore fiber amplifier," Opt. Express **19**(17), 16715–16721 (2011).
14. Y. Tshuchida, K. Maeda, K. Watanbe, T. Saito, S. Matsumoto, K. Aiso, Y. Mimura, and R. Sugizaki, "Simultaneous 7-core pumped amplification in multicore EDF through fiber based fan-in/out," in European Conference on Optical Communications, OC, Tu.4F.2 (2012).
15. K. S. Abedin, T. F. Taunay, M. Fishteyn, D. J. DiGiovanni, V. R. Supradeepa, J. M. Fini, M. F. Yan, B. Zhu, E. M. Monberg, and F. V. Dimarcello, "Cladding-pumped erbium-doped multicore fiber amplifier," Opt. Express **20**(18), 20191–20200 (2012).
16. Y. Mimura, Y. Tsuchida, K. Maeda, R. Miyabe, K. Aiso, H. Matsuura, and R. Sugizaki, "Batch multicore amplification with cladding-pumped multicore EDF," in *European Conference on Optical Communications* (2012), Tu.4.F.1.
17. D. W. Peckham, Y. Sun, A. McCurdy, and R. Lingle, Jr., "Few-mode fiber technology for spatial multiplexing," in *Optical Fiber Telecommunications Volume VI-A: Components and Subsystems,* I. P. Kaminov, T. Li, and A. E. Wilner, eds. (Elsevier, 2013), pp. 283–320.
18. K.-P. Ho and J. M. Kahn, "Frequency diversity in mode-division multiplexing systems," J. Lightwave Technol. **29**(24), 3119 (2011).
19. W. Q. Thornburg, B. J. Corrado, and X. D. Zhu, "Selective launching of higher-order modes into an optical fiber with an optical phase shifter," Opt. Lett. **19**(7), 454–456 (1994).
20. S. G. Leon-Saval, A. Argyros, and J. Bland-Hawthorn, "Photonic lanterns: a study of light propagation in multimode to single-mode converters," Opt. Express **18**(8), 8430–8439 (2010).
21. Y. Jung, Q. Kang, V. A. J. M. Sleiffer, B. Inan, M. Kuschnerov, V. Veljanovski, B. Corbett, R. Winfield, Z. Li, P. S. Teh, A. Dhar, J. Sahu, F. Poletti, S.-U. Alam, and D. J. Richardson, "Three mode Er3+ ring-doped fiber amplifier for mode-division multiplexed transmission," Opt. Express **21**(8), 10383–10392 (2013).
22. S. Jain, T. C. May-Smith, A. Dhar, A. S. Webb, M. Belal, D. J. Richardson, J. K. Sahu, and D. N. Payne, "Erbium-doped multi-element fiber amplifiers for space-division multiplexing operations," Opt. Lett. **38**(4), 582–584 (2013).
23. S. Jain, T. C. May-Smith, and J. K. Sahu, "Er/Yb-doped cladding-pumped multi-element fiber amplifier," in *Workshop on Specialty Optical Fibers and Their Applications* (2013), W5.4.
24. S. U. Alam, A. T. Harkar, R. J. Horley, F. Ghiringhelli, M. P. Varnham, P. W. Turner, and M. N. Zervas, "All-fibre, high power, cladding-pumped 1565nm MOPA using high brightness 1535nm pump sources," in *Conference on Lasers and Electro-optics* (2008), CWJ4.
25. K. H. Yla-Jarkko, C. Codemard, J. Singleton, P. W. Turner, I. Godfrey, S.-U. Alam, J. Nilsson, J. K. Sahu, and A. B. Grudinin, "Low noise intelligent cladding-pump L-band EDFA," IEEE Photonics Technol. Lett. **15**(7), 909–911 (2003).
26. S. Jain, T. C. May-Smith, V. J. F. Rancaño, P. Petropoulos, D. J. Richardson, and J. K. Sahu, "Multi-element fibre for space-division multiplexed transmission," in *European Conference on Optical Communications* (2013), Mo.4.A.2.
27. V. J. F. Rancaño, S. Jain, T. C. May-Smith, J. K. Sahu, P. Petropoulos, and D. J. Richardson, "First demonstration of amplified transmission line based on multi-element fibre technology," in *European Conference on Optical Communications* (2013), PD1.C.2.

1. Introduction

Society's ever increasing data traffic demands will eventually place a huge strain on existing and emerging networks based on standard single mode fiber (SMF) whose ultimate transmission capacity is within sight of being reached in the laboratory. Whilst this future demand might in principle be met in technical terms by installing ever more parallel SMF systems, the economics of this approach are not favorable since the cost per additional bit added will essentially be fixed once optimal spectral-efficiency transmitters and receivers are commercially deployed. Such a scenario is counter to the historic trend of operators reducing the cost-per-bit by upgrading their terminal equipment to more optimally exploit the available SMF bandwidth and scale the network capacity. Space-division multiplexing (SDM) [1,2] has emerged as a route to significantly increase per-fiber capacity and to reduce the associated costs-per-bit through the potential for device integration and sharing of expensive components, such as optical amplifiers and reconfigurable optical add drop multiplexers (ROADMs). The bulk of research on SDM has so far been focused on either multicore fiber (MCF) or multimode fiber (MMF), with impressive progress in terms of capacity enhancements demonstrated [1].

MCFs [3] comprise multiple cores in a common cladding, allowing independent parallel data transmission through the cores, thereby increasing the per-fiber capacity. However, in

#200150 - $15.00 USD Received 11 Nov 2013; revised 27 Jan 2014; accepted 4 Feb 2014; published 11 Feb 2014

MCF, the cladding diameter is restricted to ~225μm [4] by mechanical reliability considerations. This constraint, along with the minimum pitch required for low crosstalk, restricts the effective core area (A_{eff}) and the maximum number of cores that can be accommodated in an MCF design. Various geometries such as Heterogeneous [5], Homogenous [6], Trench-Assisted [7] and Hole-Assisted [8] MCFs have been investigated in order to reduce the crosstalk and increase the core-density. Currently, the maximum number of cores providing acceptably low levels of crosstalk for >100km transmission is limited to ~13 [9] due to the afore-mentioned restrictions. In addition, use of MCF requires the development of specialized components for coupling to and from the individual cores with low crosstalk [10]. Free space, integrated optic and fiber based devices are all now available but add additional cost, appreciable loss and require critical alignment [11,12]. These issues/impairments reduce the cost-advantage that MCF offers through SDM implementation. As well as passive components, there have been various demonstrations of MCF based core [13,14] and cladding-pumped amplifiers [15,16], but these devices also use couplers, as discussed above, to access the cores.

The other approach, the use of MMFs, generally supporting a few modes (i.e. Few Mode Fibers (FMFs)), allows parallel transmission channels defined by the different propagation modes [17]. However, mode coupling for long-haul transmission systems becomes inevitable in MMFs, and multi-input-multiple-output (MIMO) processing is necessary to decouple the signals. This also leads to a considerable increase in system complexity [18], as well as significant extra power consumption and cost, which need to be offset by savings elsewhere in the system to make the approach commercially viable. Furthermore, mode-dependent losses and gain cannot be fully compensated [17]. The FMF approach also requires the development of coupling components, such as photonic lanterns, to launch different modes, or at least orthogonal groups of modes, into the core [19,20]. Various amplifiers for MMF transmission lines aimed towards the reduction of mode dependent gain have been demonstrated [21].

Herein, a robust and practical approach to implement SDM based on multi-element fibers (MEFs) has been presented, which can be used to overcome many of the current limitations associated with MCF and MMF systems while, at the same time, improving the cost-efficiency. MEFs comprise multiple fiber-elements that are drawn and coated together in a common polymer coating. They allow for a more compact configuration of fibers as compared to a bundle of SMFs, allowing increased spatial channel densities, since the mechanical stiffness provided by the common coating is expected to allow the use of significantly thinner fibers than could be bundled separately due to the onset of micro-bending loss as the fiber diameter is reduced. MEFs also provide convenience in fiber handling; each fiber-element can be accessed individually by stripping-off the polymer coating, allowing conventional splicing to be used to connect to SMF components. The development of fan-in, fan-out multiplexing components is therefore not required. Moreover, as opposed to MCF, there is in principle no fundamental upper limit to the diameter of a MEF (and associated number of elements) provided that the mechanical robustness of the individual elements is maintained. This allows for larger core-to-core spacing than in MCFs thereby ensuring ultralow crosstalk and effectively independent data channels. It should also be mentioned that the high-index, highly-absorbing polymer coating between the elements further substantially reduces the potential for crosstalk.

The MEF geometry can also be easily extended to the manufacture of multi-element fiber amplifiers. We have already demonstrated core-pumped multi-element Erbium (Er) doped fiber amplifiers (ME-EDFAs), comprising 3 and 7 Er-doped fiber-elements [22]. Importantly, as shown here, a cladding-pumped Er/Yb-doped 5-element MEF amplifier (ME-EYDFA) has also now been realized [23]. In the cladding-pumped ME-EYDFA, a central fiber-element carries the pump light, which is shared between several surrounding active (signal) fibers, four in the case of the work described here. Pump sharing is critical in lowering the cost per

#200150 - $15.00 USD Received 11 Nov 2013; revised 27 Jan 2014; accepted 4 Feb 2014; published 11 Feb 2014

transmitted bit. The combination of multiple pump fibers with a single active fiber has been demonstrated previously for high power applications and L-band erbium amplifiers [24, 25]. In this paper, the MEF fabrication technique for implementing the cladding-pumped multi-element amplifier concept for SDM systems has been described. It has also been shown that multiple active fibers can be combined in series to make cascaded amplifiers, thus opening the possibility to improve the gain flatness and/or wavelength tunability.

The fabrication and characterization of both the passive MEFs [26] and the ME-EYDFA will be discussed, and also transmission experiments that combine the passive MEF fibers and the amplifier will be presented. Our experiments illustrate the functionality of the approach and demonstrate the compatibility of MEF technology with the existing SMF technology [27].

2. Passive MEF fabrication and characterization

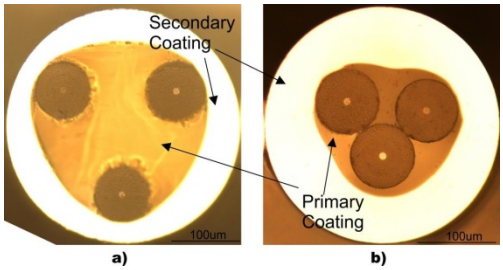

Fig. 1. Microscope image of a) non-compact and, b) compact Ge-doped 3-MEF cross-section with dual polymer coating.

Figures 1(a) and 1(b) show microscope images of the cross-section of two 3-element MEF (3-MEFs), (a) a non-compact variant (widely spaced elements) and (b) a compact variant (elements in contact), that were fabricated from a Ge-doped preform, and used in the transmission experiments. At first, a non-compact 3-MEF, with an element diameter of 80μm, was fabricated using undoped clear fused quartz (CFQ) test rods (Heraeus) to test the strength of the fibers resulting from different fabrication parameters. The fiber elements were coated together with a high-index dual polymer coating. The 3-MEF from the trial fabrication runs was then proof-tested to measure the fiber strength using an industrial fiber rewind and proof testing instrument. In our case, the required weight was scaled to accommodate for the number of elements in the MEF. The fiber passed a 400-kpsi strength test. Subsequently, a non-compact 3-MEF preform was assembled from a germanium (Ge)-doped silica preform with a core numerical aperture (NA) of 0.12, and 9.5km of 3-MEF was fabricated with cladding and core diameters of each fiber-element as ~80μm and 8.5μm respectively (see Fig. 1(a) for cross-section). The overall coated diameter was 340μm. The cut-off wavelength and measured dispersion at 1550nm of each fiber-element was approximately 1250nm and 18ps/nm/km respectively. The loss measured at 1550nm with an Exfo-FTB-7300E optical time-domain reflectometer (OTDR) was 0.6dB/km. A very similar loss was measured in a single fiber drawn from the same Ge-doped preform with single mode core and cladding diameter of 100μm. The relatively high loss as compared to SMF in this instance is thought to be due to the preform manufacture rather than the MEF fabrication process itself. We plan to use low-loss commercial grade preforms to verify this at the 0.2dB/km level. The fiber-elements were subsequently connected in series with the output of one fiber-element spliced to the input of the next, thus obtaining an effective total transmission length of 28.5km. Figure 2 compares the OTDR loss for one of the fiber-elements, named F2 (length = 9.5km), with the complete channel length obtained by looping back the fiber-elements. The loss profile along the length of the MEF was similar for all the fiber-elements. Also, no crosstalk (down to the level of −80 dB) was observed between the different fiber-elements when measured using a laser source at 1550nm.

#200150 - $15.00 USD Received 11 Nov 2013; revised 27 Jan 2014; accepted 4 Feb 2014; published 11 Feb 2014

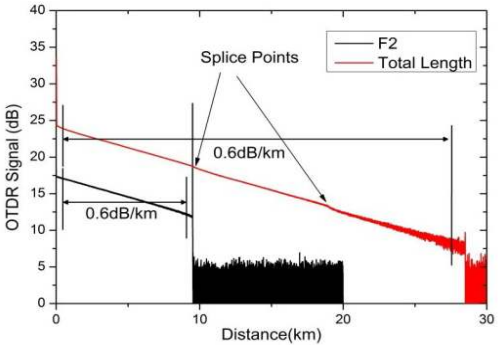

Fig. 2. OTDR loss for one of the fiber-elements (F2) and fiber-elements looped back in 3-MEF.

The 3-MEF was characterized for bit-error-rate (BER) performance using twenty-one 10-Gbit/s-OOK channels, two 40-Gbit/s-BPSK channels, and two 24-Gbit/s-QPSK channels which were wavelength multiplexed into the fiber, resulting in a data rate of 338Gbit/s per fiber-element and an overall transmission rate of 1014 Gbit/s. All the channels were determined to be error-free at the output. Negligible optical signal to noise ratio OSNR degradation and flat spectral attenuation across the 1550nm wavelength band was observed.

Similar experiments were performed on a 3.07-km length of compact 3-MEF with an overall coated diameter of 297μm, which was fabricated to increase the element density using a further section of the same Ge-doped preform. Figure 1(b) shows the cross-section image of the compact 3-MEF. The compact 3-MEF was also measured to be free from any crosstalk, and its performance was also confirmed by performing BER measurements. The same setup was used and this time the overall length was 9.1km. It was noted, however, that the loss of this 3-MEF measured at 1550nm using an OTDR was significantly higher for two of the fiber-elements than it was in the third (2.5dB/km as compared to ~0.7dB/km). It is believed that this was due to imperfect coating which also led to the fiber-elements touching and a resultant decrease in fiber strength to the 100Kpsi level. As seen in Fig. 1(b), the fiber-elements were also positioned off-center with respect to the outer coating. This problem should be readily resolved by further refining the MEF drawing process. In fact, following the experiments described in this paper, a 4.4km of 3-MEF with element separation (interstitial distance) of ~55μm, as opposed to ~95μm in non-compact 3-MEF, was fabricated which passed the same proof test level as that of the non-compact MEF. The loss observed in the fiber-elements was (0.6-0.65)dB/km, which was the same as the loss observed in the non-compact 3-MEF, confirming the scope for making the elements more compact with further optimization of the process.

3. Cladding-pumped Er/Yb-doped MEF amplifier

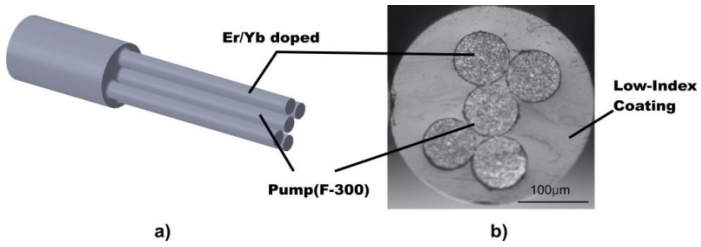

Fig. 3. a) Schematic of the 5-MEF preform assembly, and b) microscope image of the 5-MEF cross-section.

Apart from passive fibers that would be suitable for transmission, we also experimented with active fibers for the development of amplifiers. To this end, a five-element MEF (5-MEF)

#200150 - $15.00 USD Received 11 Nov 2013; revised 27 Jan 2014; accepted 4 Feb 2014; published 11 Feb 2014

was fabricated comprising four active (amplifying) elements and a core-less one for the delivery of the pump beam. The 5-MEF preform was fabricated from a high purity silica rod (Suprasil F-300) and an Er/Yb-doped preform. The Er/Yb-doped preform was cut into four equal lengths and stacked with a central silica rod to obtain the assembly shown in Fig. 3(a). The preform assembly was then drawn into fiber using a single low-index polymer coating, resulting in a calculated pump NA of 0.46. Each fiber-element had a cladding diameter of 80μm, and the core diameter in the signal fiber-elements was about 8μm. The overall coated diameter was 305μm. A microscope image of the 5-MEF cross-section is shown in Fig. 3(b). Each of the signal fiber-elements was arbitrarily labeled as S1, S2, S3 and S4 respectively, and the pump fiber-element labeled as P. The core and cladding absorption of the signal fiber-elements were measured with a white light source. Core absorption was found to be 36-61dB/m at a wavelength of 1536nm, whereas the cladding absorption was found to be 2.2-4.1dB/m at a wavelength of 975nm. The variation of rare-earth concentrations along the length of the Er/Yb-doped preform used in this work led to a variation in the absorption measured for different signal fiber-elements. This was also reflected in the refractive index profile of the preform with the index difference (Δn) varying in the range 0.011-0.015 between elements. By taking multiple cross-section images along the fiber length, it was verified that the geometry of the fiber was consistent throughout its length.

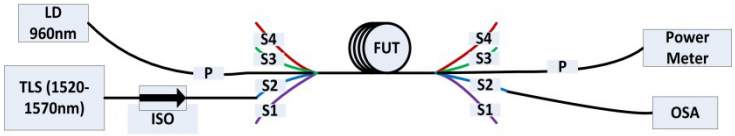

Fig. 4. Experimental setup for gain and noise figure measurements.

A 4m length of 5-MEF was taken and SMF patch cords were spliced to each end of the signal fiber-elements for gain and noise figure (NF) characterization with the experimental setup as shown in Fig. 4. The setup comprised of a multimode laser diode (LD) at a wavelength of 960nm, which was used as the pump source, a tunable laser source (TLS) as the signal source and an optical spectrum analyzer (OSA) to record the input and output signals. Figure 5(a) shows the gain and NF performance of the individual signal fibers using 6.4W of launched pump power in fiber-element P. A minimum NF of 4.7 dB with a maximum gain of 35 ± 2.5 dB was observed per signal fiber element for an input signal of −23dBm. Note that the signal fiber-elements were actually two-moded, which is likely to have contributed to the relatively higher noise figures shown in Fig. 5(a). However, SMF tails were carefully spliced to these to ensure effectively SM operation in practice, and the amplifier operated in a stable fashion with no fluctuation in its output power over time. There is no intrinsic reason that the fiber cores should be two-moded, and this issue should be readily eliminated in the next phases of fabrication work with expected improvements in amplifier performance. The maximum gain increased to 37 ± 2dB when the launched pump power was increased to 10W. The pump power vs. gain curve is plotted in Fig. 5(b) for signal fiber-elements S1 and S2 respectively, showing the gain saturation beyond about 8W of launched pump power. As in the case of the passive MEF, no signal crosstalk was observed between the signal fiber-elements above the amplified spontaneous emission (ASE) level.

#200150 - $15.00 USD Received 11 Nov 2013; revised 27 Jan 2014; accepted 4 Feb 2014; published 11 Feb 2014

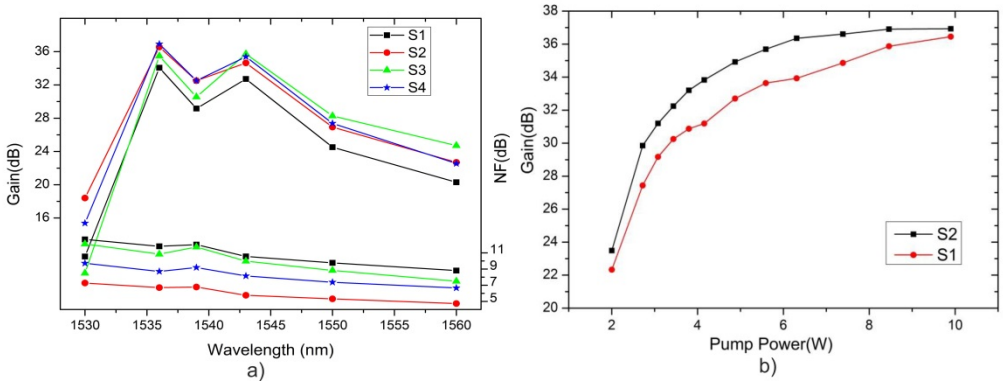

Fig. 5. a) Gain and noise figure variation with wavelength for MEF signal fibers with a pump power of 6.4W and input signal of –23dBm, and b) pump power vs. gain for –23dBm input signal at a wavelength of 1543nm for signal fibers S1 and S2 respectively.

The signal fiber-elements were connected together one by one to form a cascaded amplifier and the change in the ASE spectrum and gain was recorded as each signal fiber-element was added to investigate the gain profiling potential of the amplifier. The gain was measured with 2.5W and 4.5W of launched pump power, respectively, for the following configurations: a) S4, b) S4-S1, c) S4-S1-S2, as shown in Fig. 6(a). An input signal of –23dBm was used to measure the gain at four different wavelengths that are shown in Fig. 6(b). It was observed that the bandwidth of the cascaded amplifier increased as more signal fiber-elements were added to the device. The gain at longer wavelengths also increased significantly as more signal fiber-elements were combined. For a three-element cascaded (S4-S1-S2) amplifier, a gain of 36dB was observed over a bandwidth of >20nm with a gain flatness of ± 1dB. Also, there was a small variation in the gain profile of the amplifier depending on the cascading combination.

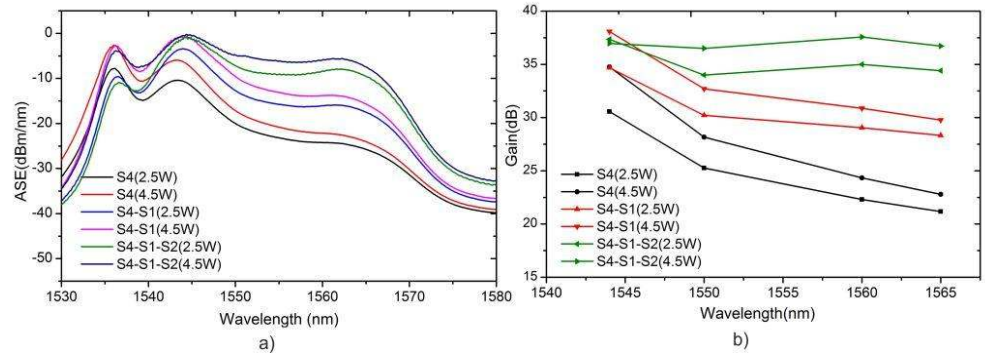

Fig. 6. Wavelength variation of a) ASE, and b) gain for different cascaded amplifier configurations.

To test the operation in a WDM environment, a source comprising 28 intensity modulated channels in the range of 1535-1562nm was used in place of the TLS in Fig. 4. The amplifier characteristics were measured, both for a single-pass configuration, as well as for different cascade configurations, for input signal powers of –6.6dBm and 0dBm, and a launched pump power of 6.4W. Figures 7(a)–7(c) show the gain and NF plots for S2, S2-S4, and S2-S4-S1 cases respectively. The gain increment at longer wavelengths was observed in the multi-channel cases, and can be clearly seen shifting from Figs. 7(a)–7(c). Figure 7(d) shows the output amplified signal spectra for S2, S2-S4 and S2-S4-S1 for 6.4W of launched pump power. The results indicate that further improvements in the amplifier characteristics can be

#200150 - $15.00 USD Received 11 Nov 2013; revised 27 Jan 2014; accepted 4 Feb 2014; published 11 Feb 2014

obtained by optimizing the amplifier length. It is also anticipated that improvements in fiber fabrication should allow for optimization of the uniformity of the amplifier element performance.

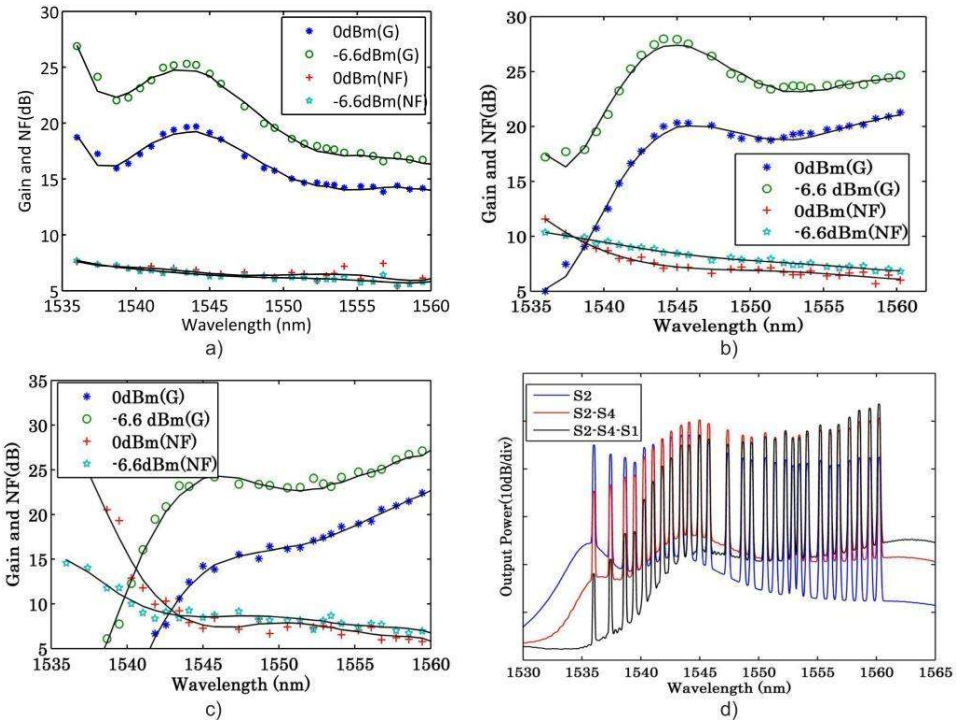

Fig. 7. Gain and NF performance of cascade combinations; a) S2, b) S2-S4, c) S2-S4-S1, and d) output spectra corresponding to three cascading cases. (Note the dots represent the experimental data and solid lines are simply trend lines to help guide the eye)

4. SDM system demonstration

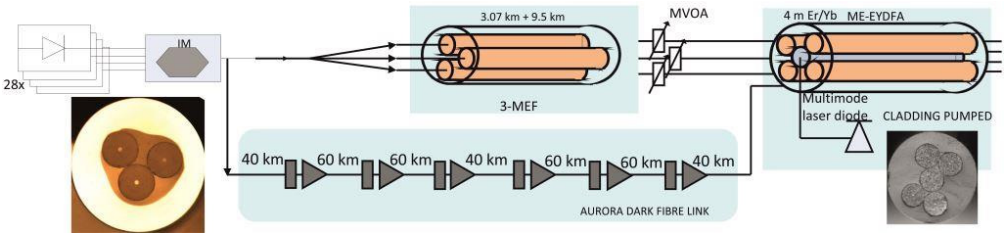

Fig. 8. Experimental set-up and cross-section of the MEF [26] and ME-EYDFA [23].

Following the characterizations of the passive 3-MEF and the 5-element ME-EYDFA in isolation, a transmission experiment was set up to emulate a hypothetical scenario of a smooth system upgrade from a single-mode WDM system to an MEF-based SDM one [27]. The experimental setup is shown in Fig. 8. The transmitter consisted of 28 channels in the range 1535nm to 1562nm, modulated using a 10Gbit/s 2^{31}-1 NRZ OOK pseudorandom bit sequence. The transmission line comprised four parallel paths, three of which were formed in the corresponding elements of a 3-MEF, whereas the fourth was a 400km dark fiber link (installed as part of the UK's AURORA network and ranging the distance from Southampton to London (Telehouse) and back). The total length of the 3-MEF was 12.57km and was made up of the two fiber lengths presented in Section 2, with respective lengths of 9.5km and 3.07km. As described previously, in order to connect the two fiber sections together, their

#200150 - $15.00 USD Received 11 Nov 2013; revised 27 Jan 2014; accepted 4 Feb 2014; published 11 Feb 2014

individual fiber-elements were simply stripped out of their protective coating at the fiber tips and spliced to standard SMF connectors using a conventional fiber splicer. The outputs of the four transmission paths with an aggregate data rate of 1120 Gbit/s were connected to the signal fiber-elements of the ME-EYDFA: the three elements of the MEF were connected to three of the input ports of the ME-EYDFA, the fourth port of which was connected to the dark fiber link (see Fig. 8). Three manual variable optical attenuators (MVOA) were installed at the input ports of the ME-EYDFA to compensate for any differences in both the attenuation of the different MEF elements and the gain of the various ME-EYDFA elements. It should be noted that the ME-EYDFA did not include any isolators or gain flattening elements (as opposed to what would be considered as normal for an amplifier used in a transmission link).

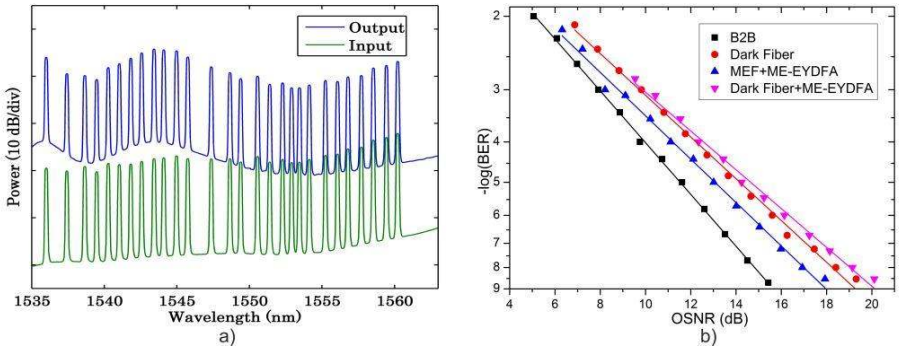

Fig. 9. a) Input and output spectra for the signals coming from the dark fiber link, and b) BER curves for the single amplification experiment.

Figure 9(a) shows the spectrum at the input and the output of the ME-EYDFA for the signal transmitted through the dark fiber link. The BER of all channels propagating through the four elements of the ME-EYDFA was assessed at the output of the amplifier and error-free trans-mission (BER<10^{-9}) was verified for both the MEF and the dark fiber paths. An example of the BER performance of the system including the ME-EYDFA for both types of paths is displayed in Fig. 9(b) (as measured for the channel operating at a wavelength of 1542nm). In order to verify that no crosstalk occurred in the ME-EYDFA, the signals at each of the ME-EYDFA output ports were characterized while the remaining fiber amplifier elements were either fed with the data signals on or off at their inputs. The OSNR of the signals was adjusted traversing one element of the ME-EYDFA in order to achieve a BER level of 10^{-8} at the output. The deviation from this BER value was then measured while successively turning on the signals in the remaining fiber elements. No change in the detected signal power and no measurable degradation in the BER of any of the assessed channels were observed, irrespective of the number of elements of the ME-EYDFA used in parallel, or their input powers, thus confirming that the various elements were completely independent from one another in terms of crosstalk, and/or cross-gain modulation effects.

Subsequently, in order to assess the performance of a chain of ME-EYDFAs, the transmission path was changed so that pairs of MEFs and ME-EYDFA spans were connected in succession, as shown in the inset of Fig. 10(a). The accumulated spectral gain ripple of the ME-EYDFA led to a gain variation of up to 15dB between the transmitted WDM channels, leading to compromised data transmission at wavelengths away from the 1545nm peak gain region. In order to demonstrate the improved performance that might be achieved by optimizing the amplifier length, the set-up was modified to exploit the gain profiling capacity of the amplifier; the second stage of amplification was made up by cascading two elements of the ME-EYDFA (see green path in the inset of Fig. 10(b)). The result is presented in Fig. 10(b), and shows a better gain equalized performance at longer wavelengths. It was

#200150 - $15.00 USD Received 11 Nov 2013; revised 27 Jan 2014; accepted 4 Feb 2014; published 11 Feb 2014

verified that by using this configuration it was possible to achieve error-free performance for all channels beyond a wavelengths of 1540nm, indicating that important performance benefits can be gained from an optimized amplifier design.

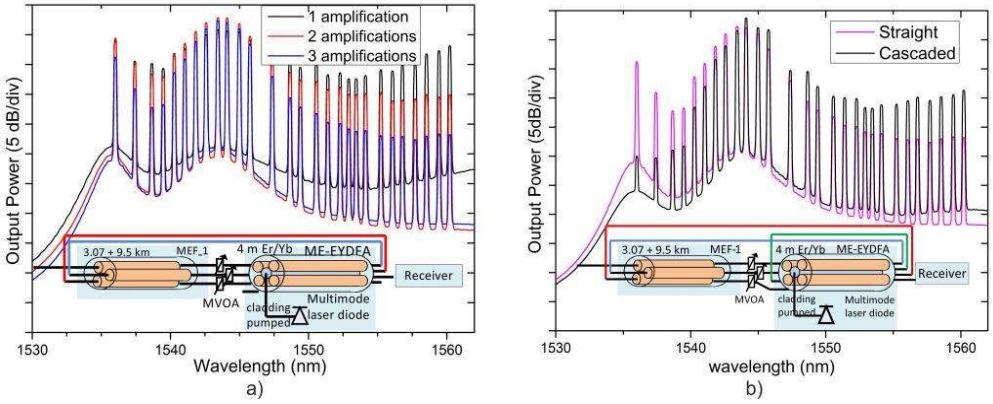

Fig. 10. Spectra a) after three amplifications with three single-stage ME-EYDFA, and b) with two single stage amplifiers and a dual-stage amplifier.

5. Conclusions

A novel approach to implementing SDM transmission based on multi-element fiber technology is presented. MEFs offer effectively crosstalk-free operation, compatibility with conventional WDM systems and do not require the development of any special multiplexing components. MEF technology enables multiple fibers to be drawn together within a common coating, and can be applied to the manufacturing of both passive transmission fibers and active fibers for the development of amplifying modules. The feasibility of this approach was demonstrated by fabricating and characterizing 9.5km and 3.07km lengths of a passive 3-MEF from a Ge-doped preform. Error-free 1014Gbps data transmission over the lengths of MEF was demonstrated, highlighting the crosstalk-free operation obtained. A cladding pump ME-EYDFA was also demonstrated, which shares a single pump for the simultaneous amplification of four independent Er/Yb-doped fiber-elements. A maximum gain of 37 ± 2 dB per fiber-element for 10W of launched pump power and −23dBm input signal was obtained. Our ME-EYDFA had a length of 4m, whereas by cascading fiber-elements together, the potential of adjusting the gain profile of the amplifier was demonstrated. Finally, the first implementation of an amplified MEF-based SDM transmission system including both passive and active SDM components was experimentally demonstrated. The MEF technology shows full compatibility with existing WDM systems and sufficient flexibility to be considered as a contender for the implementation of fully functional SDM systems.

Acknowledgments

This work was supported by the EPSRC grant EP/I01196X: Transforming the Future Internet: The Photonics Hyperhighway. The authors thank JANET, the UK's research and education network, for gratefully providing the installed fiber link used during these experiments. The authors are thankful to Dr. Sumiaty Ambran and Dr. Ming Ding for their help with obtaining microscope images of the MEF and for tapering of pump-delivery fibers.